Journal of Membrane Science 452 (2014) 453–459

Contents lists available at ScienceDirect

Journal of Membrane Science

journal homepage: www.elsevier.com/locate/memsci

Mathematical sigmoid-model approach for the determination of limiting and over-limiting current density values

Alain Doyen [a,b], Cyril Roblet [a,b], Adam L'Archevêque-Gaudet [c], Laurent Bazinet [a,b,*]

[a] Institute of Nutrition and Functional Foods (INAF), Université Laval, Québec, QC, Canada G1V 0A6
[b] Department of Food Science and Nutrition, Université Laval, Québec, QC, Canada G1V 0A6
[c] Department of Mathematics, Collège d'enseignement général et professionnel (CEGEP) de Lanaudière, Joliette, QC, Canada J6E 4T1

ARTICLE INFO

Article history:
Received 9 September 2013
Received in revised form
28 October 2013
Accepted 29 October 2013
Available online 19 November 2013

Keywords:
Limiting current density determinations
Sigmoidal curve
Potential difference
Ion-exchange membrane
Ultrafiltration membrane

ABSTRACT

The effect of successive limiting current density (LCD) determination procedures on electrodialysis with ultrafiltration membrane (EDUF) system was studied in order to evaluate their impact on ion-exchange (IEM) and ultrafiltration membranes (UFM) integrity by measuring *in situ* the membrane potential difference. In the first protocol, two successive LCD determination procedures were carried-out by increasing the voltage by 2 V from 0 to 40 V, spaced by a rest period of 60 min. In the second protocol, the LCD determination procedures were performed every 20 min during 60 min. For both protocols, voltage–current curves were plotted for IEM and UFM and I_{lim} values were determined. Results showed that only anion-exchange membrane (AEM) showed a typical sigmoidal curve for both protocols. Moreover, it was demonstrated that a rest time period of 60 min between two successive LCD determination procedures had no impact on system current density and membrane potential difference while four successive LCD determinations spaced by a constant rest period of 20 min allowed delaying the appearance of I_{lim} and over-limiting current region. A mathematical sigmoid-model approach was also proposed allowing for the first time the calculation of the different parameters typical of water splitting phenomenon from a voltage–current curve.

1. Introduction

Electrodialysis (ED) is defined as an electrochemical separation process used to separate ionic species from an aqueous solution and other uncharged components [1]. Several design parameters such as feed flow velocities, ion concentrations and stack design affect the performance of ED system and contribute to the appearance of concentration polarization phenomenon at the surface of ion-exchange membranes (IEM) resulting in the appearance of limiting current density (LCD) [2]. During conventional electrodialysis experiment, LCD appears since the concentration of ion species at the surface of the cation-exchange membrane (CEM) and/or anion exchange membranes (AEM) in the depleted solution (diluate) compartment reached zero [3]. Consequences of LCD phenomenon are water molecule dissociation, salt precipitation and drastic changes of ED system performances [4]. Consequently, LCD represents a key parameter to control and, its determination before ED experiments is primordial.

In this context, practical and mathematical methods were developed and used to determine or estimate the limiting current density value (I_{lim}). Hence, Cowan and Brown [5] proposed a graphical method to determine the LCD value by quickly increasing the voltage applied to the electrodes of the electrodialysis system and recording the corresponding current density. The global system resistance was then plotted *versus* the reciprocal of the current intensity ($1/I$). At the inflection point on this graph, the current intensity divided by the membrane area is considered as the I_{lim} value of the system. Another method, reported in the literature [6–10] consists in plotting typical current–voltage data to determine graphically the I_{lim} value. The curve could be separated into three specific regions. Region I represents a linear relationship between current and voltage and referred to the ohmic region. Region II, named limiting current region, is characterized by a plateau caused by ion-depletion in the hydrodynamic boundary layer. Finally, region II is followed by the electro-convection or over-limiting current region (OLCR) (region III) in which the slope of the current–potential curve increases again [6–10]. For this type of curve, I_{lim} value is the inflection point

Abbreviations: AEM, anion-exchange membrane; CEM, cation-exchange membrane; ED, electrodialysis; EDUF, electrodialysis with ultrafiltration membranes; IEM, ion-exchange membrane; LCD, limiting current density; LCR, limiting current region; MWCO, molecular weight cut-off; OLCR, over-limiting current region; UFM, ultrafiltration membrane

* Corresponding author at: Université Laval, Institute of Nutrition and Functional Foods (INAF), Department of Food Science and Nutrition, 2425 rue de l'Agriculture, Québec, QC, Canada G1V 0A6. Tel.: +1 418 656 2131x7445; fax: +1 418 656 3353.
E-mail address: Laurent.Bazinet@fsaa.ulaval.ca (L. Bazinet).

0376-7388/$ - see front matter © 2013 Elsevier B.V. All rights reserved.
http://dx.doi.org/10.1016/j.memsci.2013.10.069

of the two slopes belonging to the ohmic and the plateau region [8,11–14]. The mathematical approach used for the determination of I_{lim} of an ion-exchange membrane (AEM or CEM) is based on the Nernst-diffusion model and is represented as

$$I_{lim} = \frac{FDC}{\delta(\bar{t}_i - t_i)} \quad (1)$$

where F represents the Faraday constant ($A\,s\,eq^{-1}$), D the salt diffusion coefficient, C the bulk solution concentration, δ the diffusion boundary layer thickness, $\bar{t}_i$ the electromigration number of counter ion in the membrane and t_i the transport number in the solution [12,15]. However, in practice, it is very difficult to determine the thickness of the diffusion boundary layer (δ) but some methods, such as chronopotentiometry [16], laser interferometry [17] or optical systems [18], were successfully used to observe and characterize it.

Although observed for conventional ED, LCD impact on electrodialysis with ultrafiltration membranes (EDUF) system is still unknown. Indeed, typically before EDUF experiments, a constant voltage difference was determined according to the Cowan and Brown method [5] to limit water splitting and pH fluctuations. In addition, the impact of successive LCD determination procedures on IEM and UFM stacked in an ED or EDUF system has never been studied. Consequently, the objectives of the present work were (1) to apply successive LCD determination procedures on EDUF system with constant rest times, (2) to evaluate the impact of these successive LCD determination procedures on IEM and UFM integrity and (3) to propose a mathematical model allowing the calculation of I_{lim} value and other parameters.

2. Materials and methods

2.1. Chemicals

HCl and NaOH 1.0 M solutions were obtained from Fisher Scientific (Montreal, QC, Canada). NaCl and Na_2SO_4 were purchased from Laboratoire MAT (Québec, QC, Canada). KCl was purchased from ACP Inc (Montreal, QC, Canada).

2.2. Raw material

The snow crab by-products hydrolysate was obtained from Merinov (MAPAQ, Gaspé, QC, Canada). The hydrolysate was elaborated according to a procedure described previously [19]. The initial concentration of peptides in the snow crab hydrolysate was 100 g/L (10% w/w). The water content was 87%, ash was 2.12% and lipids were below detection level.

2.3. Electrodialysis cells and configuration

The electrodialysis (ED) cell used was a EUR-2C cell (200 cm^2 of effective surface area) manufactured by Eurodia Company (Wissous, France). The EDUF cell configuration was the same as the one described by Doyen et al. [20]. Briefly, the cell configuration consisted of three Neosepta CMX-SB cationic membrane (Tokuyama Soda Ltd, Tokyo, Japan), one Neosepta AMX-SB anionic membrane (Tokuyama Soda Ltd, Tokyo, Japan) and six polyethersulfone ultrafiltration membranes (UFMs) with molecular weight cut-off (MWCO) of 20 kDa (GE, France) (Fig. 1). The compartments defined four closed loops containing the feed solution (snow crab hydrolysate), a potassium chloride solution (2 g/L KCl) for the recovery of anionic (compartment named KCl1) or cationic peptides (compartment named KCl2) and an electrolyte solution (20 g/L Na_2SO_4) for rinsing both electrode compartments. Each closed loop was connected to a separate external reservoir to allow continuous recirculation of the solutions. The KCl and feed solution flow rates were 1 L/min while the flow rate of the electrode solution was 3 L/min.

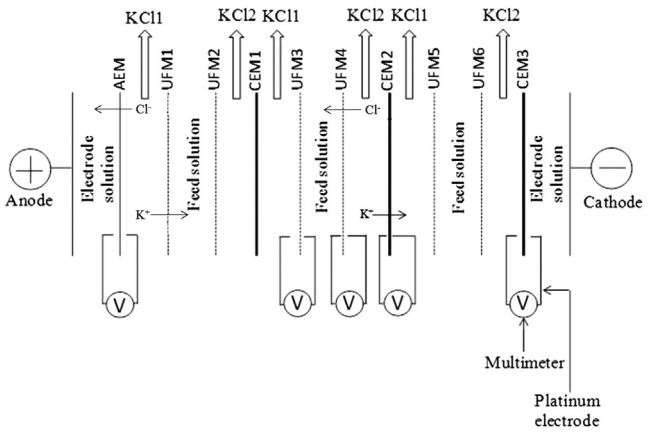

Fig. 1. Configuration of the electrodialysis with ultrafiltration membranes cell. UFM: ultrafiltration membrane. AEM: anion-exchange membrane. CEM: cation-exchange membrane.

2.4. Potential difference measurements

Electrical potential difference measurements during EDUF experiments were performed according to Doyen et al. [20] and Ling Teng Shee et al. [21]. Briefly, five platinum (Pt) electrodes pairs (GoodFellow, Huntingdon, UK), covered with silver at their ends, were disposed at membrane interfaces (Fig. 1). The ends of electrodes were in contact with the different membranes. Each Pt electrode pair was connected to a digital multimeter.

2.5. Limiting current density measurements

Two protocols were used to determine the effect of successive LCD determination procedures on IEMs and UFMs integrity. The first protocol, repeated three times, was achieved by increasing the voltage by 2 V from 0 to 40 V. At every voltage increment, the electrical potential differences of IEM and UFM and the corresponding intensity values were recorded. Afterwards, the EDUF system was left to rest during 60 min and another LCD determination procedure was performed as previously. The second protocol, also repeated three times, was the same as the previously described except for LCD determination procedure which was performed every 20 min during 60 min. For both protocols, electroseparations were performed at pH 9 since this value allowed the highest peptide recovery [20]. The pH of hydrolysate and permeate solutions (KCl1 and KCl2) was adjusted at pH 9 before each run with 1.0 M NaOH and maintained during EDUF process to avoid retromigration phenomenon. Finally, new snow crab by-products hydrolysate and KCl solutions were used after each repetition for both protocols.

2.6. Statistical analyses

The current densities and membrane potential differences obtained at 0 and 60 min during the first experiment were subjected to a nonparametric comparisons t-test ($P < 0.05$ as probability level for acceptance) while these parameters obtained at 0, 20, 40 and 60 min for the second experiment were subjected to a repeated measure analysis of variance (ANOVA, LSD (Least Significant Difference) $P < 0.05$ as probability level for acceptance) using SAS software version 9.1 (SAS Institute Inc, Cary, North Carolina, USA). Finally, I_{lim} and I_{olc} values determined by the

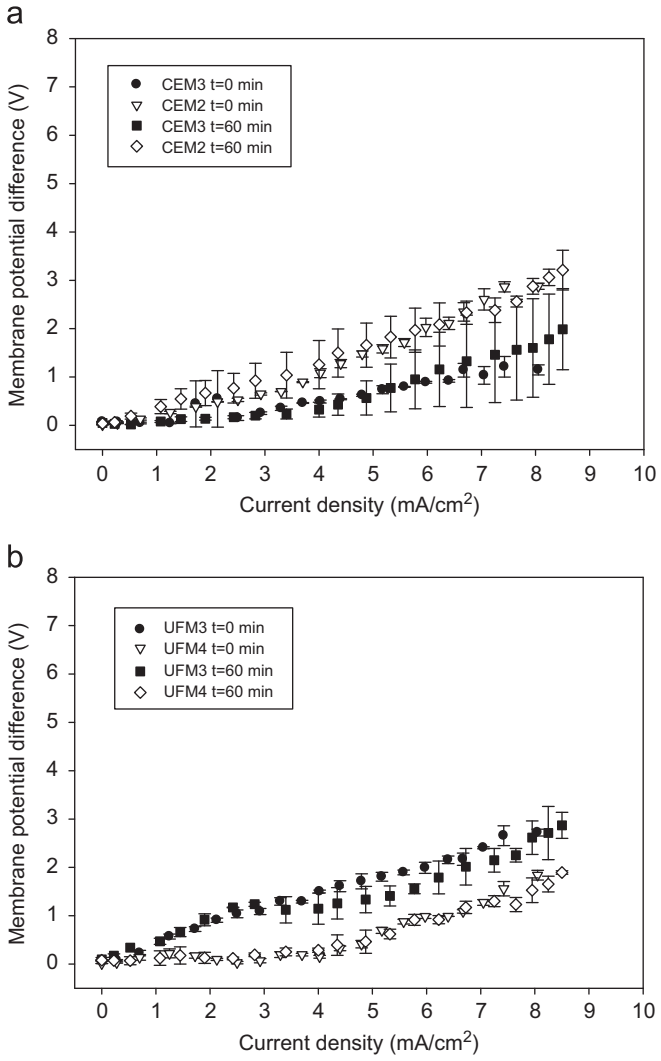

Fig. 2. Evolution of the potential difference (V) for (a) CEM2, CEM3 and (b) UFM3, UFM4 after two LCD determination procedures spaced by a rest period of 60 min.

mathematical approach proposed as well as graphically obtained from Cowan and Brown and tangent methods were also subjected to a repeated measure analysis of variance (ANOVA, LSD $P<0.05$ as probability level for acceptance) using SAS software version 9.1.

3. Results and discussion

3.1. Limiting current density measurements

3.1.1. Evolution of CEM, AEM and UFM potential differences after two LCD determination procedures spaced by a rest period of 60 min

No difference, regarding the evolution of electrical potential differences, was observed for UFM3, UFM4, CEM2 and CEM3 after the application of two LCD determination procedures spaced by a 60-min rest period (Fig. 2a and b). Indeed, the increase in the membrane potential difference was linear and after the first LCD determination procedure, CEM and UFM regained their initial potential difference values after 60 min of rest time. Consequently, the UFM and CEM integrities were not affected. However, specifically for UFMs, Fig. 2b shows that potential difference of UFM3 was higher that UFM4 whatever time of LCD determination procedures applied ($t=0$ or $t=60$ min). This result could be explained by the position of the filtration layer. Indeed, according to Fig. 1, the filtration layer of the UFM3 was facing the cathode while for the UFM4, it was facing the anode. Thus, the filtration layer can slow down the migration of ions since material which composed filtering and non-filtering layer is different in terms of composition and ion permeability, but no studies on this subject in the literature have been published.

The evolution of the AEM potential difference was different and showed a typical sigmoidal shape (Fig. 3). These data were fitted using Sigmaplot 12.0 (Systat Software, Inc., San Jose, California, USA) and the equation (Eq. (2)) used to obtain sigmoidal curves was adapted from Bazinet et al. [22]:

$$y = f(x) = y_0 + \frac{a}{1+e^{(-(x-x_0)/b)}} \quad (2)$$

where y is the membrane electrical potential difference (V), y_0 the initial value of membrane potential difference without current application (V), x the current density value (mA/cm^2), a the amplitude of the curve (V), x_0 the center or inflection point of curve (mA/cm^2) and b is the slope of the sigmoidal curve at x_0 (V mA cm^{-2}) (Fig. 4). The sigmoidal curves obtained in Fig. 3 could be separated, as reported in the literature [6–10] in three typical regions: ohmic (I), limiting current (II) and over-limiting current region (III) (OLCR) (Fig. 4). The following mathematical model was

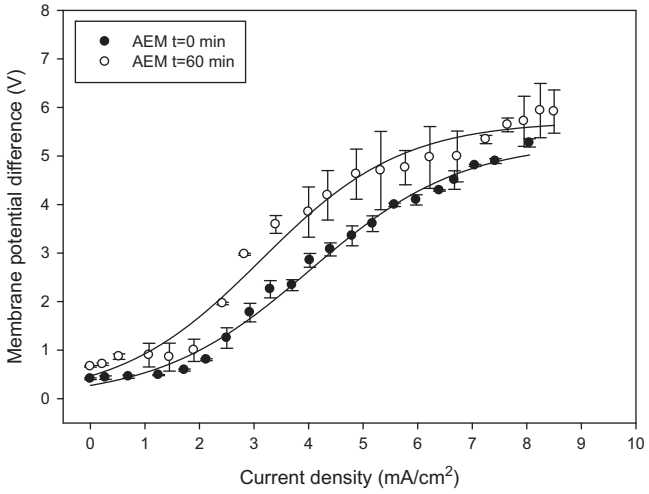

Fig. 3. Evolution of AEM potential differences after two LCD determination procedures spaced by a rest period of 60 min.

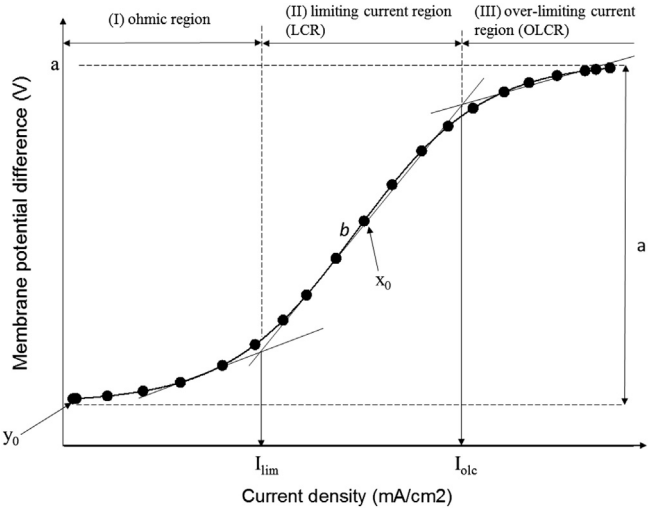

Fig. 4. Model curve for the determination of sigmoidal and electrodialytic parameters.

proposed to find I_{lim} (mA/cm^2) value:

$$I_{lim} = x_0 - (b \ln(2+\sqrt{3})) \quad (3)$$

where x_0 and b were obtained from Eq. (2)

Eq. (3) was obtained after third derivative (Eq. (4)) calculation from Eq. (2):

$$\frac{d^3}{dx^3}(f(x)) = \frac{6a(e^{(-(x-x_0)/b)})^3}{(1+e^{(-(x-x_0)/b)})^4 b^3} - \frac{6a(e^{(-(x-x_0)/b)})^2}{(1+e^{(-(x-x_0)/b)})^3 b^3} + \frac{a(e^{(-(x-x_0)/b)})}{(1+e^{(-(x-x_0)/b)})^2 b^3} \quad (4)$$

Table 1
Anion-exchange membrane parameters obtained after two LCD determination procedures spaced by a rest period of 60 min.

	Current density applications	
	t=0 min	t=60 min
R^2	0.9918 ± 0.0052	0.9799 ± 0.0073
b (V mA/cm^2)	1.45 ± 0.25[a]	1.26 ± 0.21[a]
x_0 (mA/cm^2)	4.01 ± 0.55[a]	3.15 ± 0.88[a]
I_{lim} (mA/cm^2)	2.10 ± 0.45[a]	1.49 ± 0.37[a]
I_{olc} (mA/cm^2)	5.92 ± 0.50[a]	4.81 ± 0.62[a]
Limiting current region length (mA/cm^2)	3.82 ± 0.48[a]	3.32 ± 0.50[a]
Membrane potential difference (V)	1.07 ± 0.03[a]	1.20 ± 0.26[a]

Statistical significance is indicated by letter 'a'; $P < 0.05$, nonparametric comparison t-test.

Thus, when the third derivative (Eq. (4)) is equal to zero, the critical x point (mA/cm^2) corresponds to the maximum of the second derivative (Eq. (5)). This maximum value of the second derivative corresponds to the change in slope observed on the sigmoidal curve between regions 1 and 2.

$$\frac{d^2}{dx^2}(f(x)) = \frac{2a(e^{(-(x-x_0)/b)})^2}{(1+e^{(-(x-x_0)/b)})^3 b^2} - \frac{a(e^{(-(x-x_0)/b)})}{(1+e^{(-(x-x_0)/b)})^2 b^2} \quad (5)$$

Consequently, since this x value (mA/cm^2) is the inflection point between regions I and II, it also represents a good estimation of the I_{lim} value as generally determined graphically by the cross-point of the tangents drawn from ohmic and limiting current region.

Moreover, using the sigmoidal model, the determination of I_{lim} value could be used to determine the overlimiting current density value (I_{olc}). Indeed, since a sigmoidal curve is symmetrical on each side of the inflexion point x_0 (mA/cm^2), the point corresponding to the change in slope between regions II and III and on the sigmoidal curve, called I_{olc} (mA/cm^2), was calculated by the following equation (Fig. 4):

$$I_{olc} = I_{lim} + 2(x_0 - I_{lim}) = 2x_0 - I_{lim} \quad (6)$$

Consequently, I_{olc} value obtained from Eq. (6) allowed also calculating the length of the limiting current region (LCR) (mA/cm^2) by the following equation (Fig. 4):

$$LCR = I_{olc} - I_{lim} \quad (7)$$

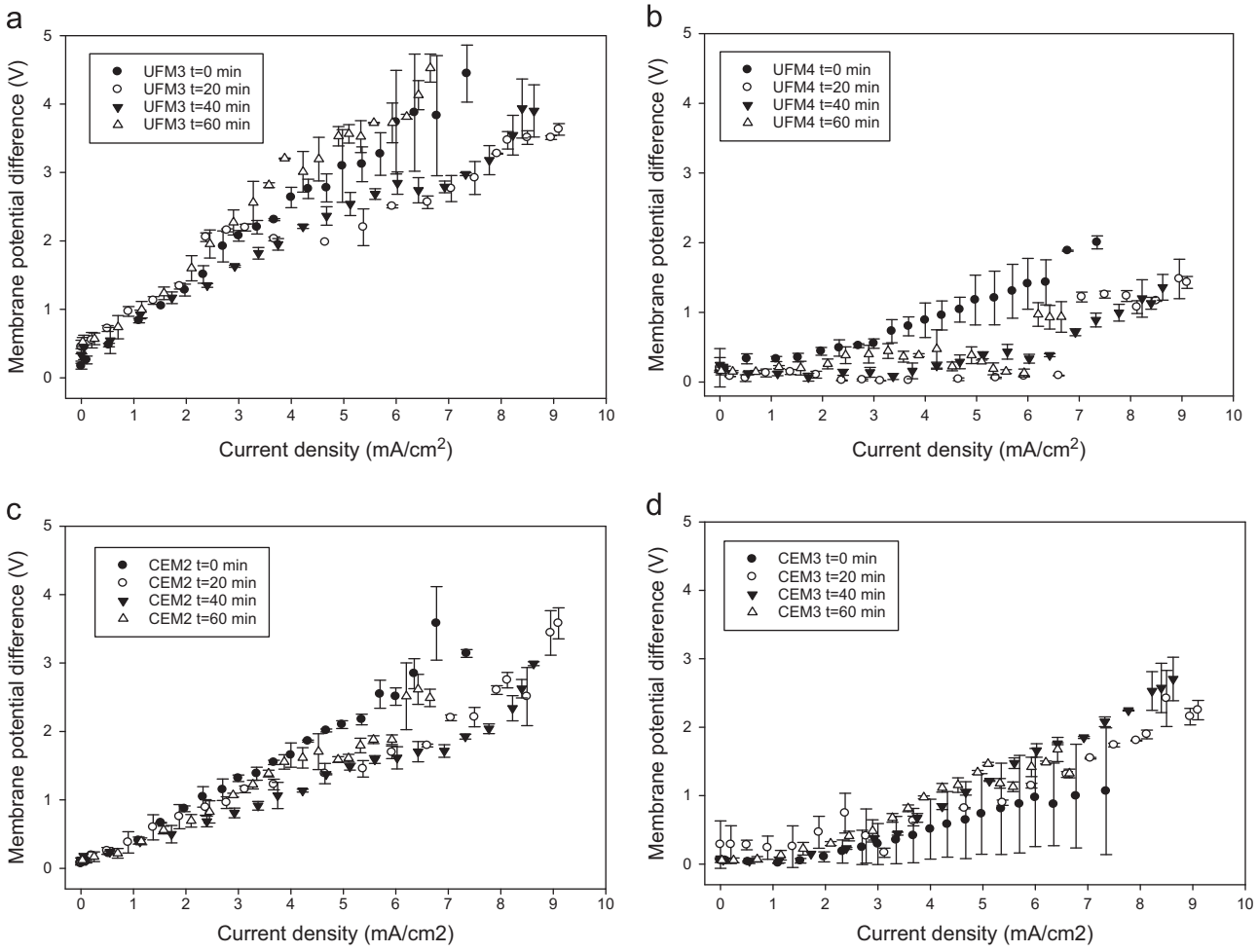

Fig. 5. Evolution of (a) UFM3, (b) UFM4, (c) CEM2 and (d) CEM3 potential differences as a function of the current density after LCD determination procedures every 20 min during 60 min.

From Eqs. (3), (6) and (7), I_{lim} and I_{olc} values were determined for AEM at $t=0$ and 60 min (Table 1). It appeared that I_{lim} calculated from the proposed model were similar between $t=0$ and $t=60$ min as well as for I_{olc} and LCR length values (Table 1). Moreover, no significant difference were observed for membrane potential difference between $t=0$ and $t=60$ min (Table 1). Consequently, a rest time of 60 min is sufficient to restore AEM to its initial potential. Thus, while AEM was highly polarized due to water dissociation and the generation of H^+ and OH^- ions after the first LCD determination, the 60 min of rest time allowed depolarizing gradually AEM to return to its initial potential difference value. Consequently, the second LCD determination, applied after 60 min of rest time, polarized the AEM at a similar level to that observed after the first LCD determination. However, with respect to the EDUF experiments, the duration between the determination of LCD by the method of Cowan and Brown [11] and the beginning of hydrolysate separation is generally less than 60 min. Thus, applications of LCD every 20 min during 60 min were performed to determine the impact of a short rest time between LCD determination procedure and the experimental EDUF run on membrane behavior.

3.1.2. *Evolution of CEM, AEM and UFM potential differences after successive LCD determination procedures every 20 min during 60 min*

The evolution of potential differences observed for the UFM3, UFM4, CEM2 and CEM3 after applications of LCD determination procedures every 20 min during 60 min was similar (Fig. 5). Indeed, whatever the type of membrane stacked in the system (CEM and UFM) and the rest period, the membrane potential difference increased when current density increased. This phenomenon is probably due to the difference of positive and negative ion charges at CEM and UFM interfaces during EDUF process resulting of a small potential difference appearance. However, as observed in Fig. 2b, membrane potential difference of UFM3 was higher than UFM4 whatever the time of LCD determination procedure ($t=0$, 20, 40 and 60 min) (Fig. 5a and b). As explained previously (Section 3.1.1), this result could be explained by the position of the filtration layer. Contrary to UFM and CEM, differences in potential differences were observed as previously for the AEM (Fig. 6) since the different curves represent typically the model observed in the first experiment. To determine if successive LCD determination procedures had significant impact on AEM integrity, membrane parameters values (I_{lim}, I_{olc}, membrane potential difference and LCR length) at $t=0$, 20, 40 and 60 min, were calculated according to Eqs. (2), (3), (6) and (7), and presented in Table 2.

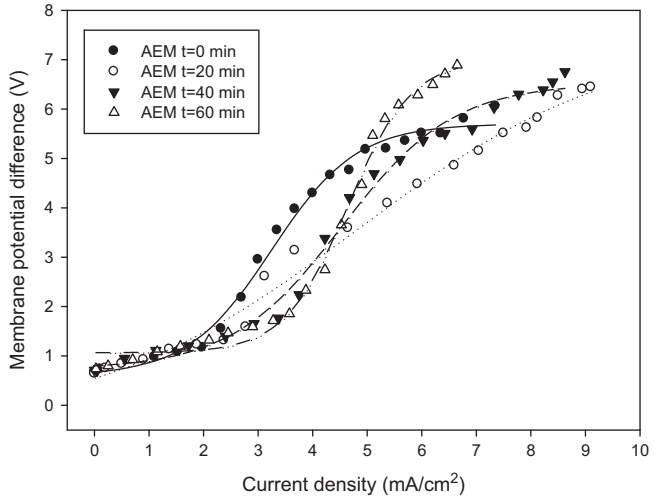

Fig. 6. Evolution of AEM potential differences, after LCD determination procedures spaced by 20 min of rest period (standard deviations were removed to avoid cluttering the figure).

Significant difference ($P<0.05$) were observed for I_{lim} whatever the period of rest time after successive LCD determinations. However, while I_{lim} increased continually at $t=0$, 40 and 60 min, a decrease was observed between $t=0$ and $t=20$ min (Table 2) and, in the same time, AEM membrane potential differences were similar at $t=0$ and 20 min but increased continually from $t=40$ until $t=60$ min ($P<0.05$). Contrary to I_{lim}, I_{olc} increased between $t=0$ and $t=20$ min but remained stable at $t=40$ and $t=60$ min (Table 2) with the consequence that LCR length was longer at $t=20$ min compared to $t=0$ min ($P<0.05$), remained stable at $t=40$ min and decreased at $t=60$ min to a value similar to that observed initially, after the first LCD determination. Consequently, these results demonstrated that successive LCD determinations spaced by rest time of 20 min allowed delaying the appearance of water splitting phenomenon and a rest period of 20 min between each LCD determination was not sufficient to depolarized AEM until its initial potential difference. Moreover, the increase of LCR length at $t=0$ and $t=20$ min allowed delaying the appearance of over-limiting current region which is considered as a dangerous stage for ED process due to the high working current [23].

3.1.3. *Validation of the mathematical approach proposed*

Values of I_{lim} and I_{olc}, obtained with the mathematical approach proposed, were compared to I_{lim} and I_{olc} values graphically determined by using the tangent and Cowan and Brown methods described in Section 1 (Table 3). However, with Cowan and Brown method, only the I_{lim} value was determined since this method allows only the determination of the limiting current density in the global electrodialytic system.

Concerning I_{lim} and I_{olc} values obtained after LCD determination procedures at $t=0$ and 60 min, no significant difference ($P>0.05$) was observed whatever the applicable method used (Table 3). Similarly, I_{lim} and I_{olc} values obtained after LCD determination procedures every 20 min during 60 min and calculated

Table 2
Anion-exchange membrane parameters obtained after LCD determination procedures every 20 min during 60 min.

	Current density applications			
	$t=0$ min	$t=20$ min	$t=40$ min	$t=60$ min
R^2	0.9928 ± 0.0039	0.9903 ± 0.0087	0.9907 ± 0.0064	0.9935 ± 0.0046
b (V mA/cm^2)	0.78 ± 0.13^{a}	0.26 ± 0.19^{b}	1.02 ± 0.23^{c}	0.58 ± 0.14^{d}
x_0 (mA/cm^2)	3.25 ± 0.14^{a}	4.77 ± 0.36^{b}	4.54 ± 0.22^{b}	4.65 ± 0.37^{b}
I_{lim} (mA/cm2)	2.23 ± 0.12^{a}	1.60 ± 0.15^{b}	3.19 ± 0.11^{c}	3.88 ± 0.09^{d}
I_{olc} (mA/cm^2)	4.27 ± 0.28^{a}	7.94 ± 0.84^{b}	5.89 ± 0.45^{c}	5.42 ± 0.38^{c}
Limiting current region length (mA/cm^2)	$2.04 \pm 0.34^{a,c}$	3.17 ± 0.49^{b}	$2.70 \pm 0.54^{a,b}$	1.54 ± 0.38^{c}
Membrane potential difference (V)	5.98 ± 0.38^{a}	6.37 ± 0.47^{a}	7.73 ± 0.54^{b}	8.52 ± 0.26^{c}

Statistical significance is indicated by different letters; $P<0.05$ one-way ANOVA and *a posteriori* Tukey test.

Table 3
Values of I_{lim} and I_{olc} determined by the mathematical sigmoid-model approach proposed as well as graphically obtained with Cowan and Brown and tangent methods.

	LCD determination procedures at $t=0$ and 60 min						LCD determination procedures every 20 min during 60 min											
	$t=0$ min			$t=60$ min			$t=0$ min			$t=20$ min			$t=40$ min			$t=60$ min		
	I_{lim}[1]	I_{olc}[1]	LCR length[1]	I_{lim}	I_{olc}	LCR length[1]	I_{lim}	I_{olc}	LCR length[1]	I_{lim}	I_{olc}	LCR length[1]	I_{lim}	I_{olc}	LCR length[1]	I_{lim}	I_{olc}	LCR length[1]
Mathematical approach	2.10 ± 0.45^a	5.92 ± 0.50^a	3.82 ± 0.48^a	1.49 ± 0.37^a	4.81 ± 0.62^a	3.32 ± 0.50^a	2.23 ± 0.12^a	4.27 ± 0.28^a	2.04 ± 0.34^a	1.60 ± 0.15^a	7.94 ± 0.84^a	3.17 ± 0.49^a	3.19 ± 0.11^a	5.89 ± 0.45^a	2.70 ± 0.54^a	3.88 ± 0.09^a	5.42 ± 0.38^a	1.54 ± 0.38^c
Cowan and Brown	2.26 ± 0.52^a			1.69 ± 0.42^a			2.04 ± 0.35^a			7.35 ± 2.46^b			2.96 ± 057^a			2.15 ± 0.69^b		
Tangent method	1.92 ± 0.37^a	5.77 ± 1.23^a	3.85 ± 0.71^a	1.75 ± 0.62^a	4.17 ± 0.83^a	2.42 ± 0.76^b	2.07 ± 0.48^a	4.58 ± 0.36^a	2.51 ± 0.81^a	1.36 ± 0.29^a	7.71 ± 0.91^a	6.35 ± 1.14^b	3.31 ± 0.61^a	5.21 ± 0.77^a	1.90 ± 0.81^b	3.61 ± 0.52^a	5.67 ± 0.41^a	2.06 ± 0.57^b

[a,bc] Statistical significance is indicated by different letters; $P < 0.05$ one-way ANOVA and *a posteriori* Tukey test.
[1] Expressed in mA/cm^2.

from our proposed approach, were not significantly different at $t=0$ and $t=40$ min from those respectively obtained by Cowan and Brown and tangent methods for I_{lim} and for tangent method for I_{olc}. However, at $t=20$ and 60 min, while I_{lim} and I_{olc} were not significantly different ($P > 0.05$) between the proposed mathematical approach and the tangent method, it appeared that I_{lim} values obtained graphically with Cowan and Brown method was statistically different ($P < 0.05$) compared to the other two methods. This difference could be explained by the atypical curve obtained at $t=20$ min during successive LCD determination procedures every 20 min during 60 min (Fig. 6). Moreover, contrary to the mathematical approach and tangent method where I_{lim} values were calculated specifically from membrane potential difference, I_{lim} obtained with Cowan and Brown method was determined on the electrodialytic system and not at the membrane interfaces. Thus, Cowan and Brown method seemed to be less precise than other methods described in this work. Consequently, the mathematical model described and proposed in this work appeared to be a valuable approach for the determination of water splitting phenomenon appearance and the calculation of voltage–current curve parameters defining the three specific regions.

4. Conclusion

Successive LCD determination procedures spaced by specific rest time periods appeared to have a significant impact on AEM integrity. Indeed, while two successive LCD determination procedures spaced by a rest period of 60 min did not affect AEM parameters (I_{lim}, membrane potential difference and LCR length), four successive LCD determination procedures spaced by a rest time of 20 min allowed delaying the appearance of limiting current density phenomenon. In the second case, I_{lim} values increased continually during consecutive procedures due to gradual polarization of AEM. Moreover, the increase of LCR length at $t=0$ and $t=20$ min allowed delaying the appearance of over-limiting current region considered as a dangerous stage due to the high working current.

While water dissociation phenomenon was suspected in previous EDUF experiments *via* pH measurements [24,25], it was the first time that it is demonstrated *in situ* and that the membrane responsible for it was identified. Moreover, this work proposed for the first time a new and valuable mathematical approach for the calculation of I_{lim}, I_{olc} and LCR length related with water splitting phenomenon. This mathematical approach could be easily applied to membrane used in all electro-membrane systems.

Acknowledgment

The authors thank Ms. Monica Araya-Farias and Diane Gagnon for their technical support. Eurodia Industries S.A (Wissous, France) is acknowledged for providing us with the commercial ultrafiltration membranes and semi-pilot ED system. A special thank to the research team of Merinov (Gaspé, QC, Canada) especially Mr. Piotr Bryl for the preparation of the hydrolysate. This research was financially supported by the Ministère de l'Agriculture des Pêcheries et de l'Alimentation du Québec (MAPAQ) and the Natural Sciences and Engineering Research Council of Canada (NSERC). Alain Doyen received a grant from NSERC-FAST (Food Advancement through Science and Training) Program Scholarship.

References

[1] V.A. Shaposhnik, K. Kesore, An early history of electrodialysis with permselective membranes, J. Membr. Sci. 136 (1997) 35–39.

[2] H.J. Lee, H. Strathmann, S.H. Moon, Determination of the limiting current density in electrodialysis desalination as an empirical function of linear velocity, Desalination 190 (2006) 43–50.
[3] Y. Tanaka, M. Iwahashi, M. Kogure, Distribution of electrodialytic condition in an electrodialyzer and limiting current density, J. Membr. Sci. 92 (1994) 217–228.
[4] Y. Tanaka, Current density distribution, limiting current density and saturation current density in an ion-exchange membrane electrodialyzer, J. Membr. Sci. 210 (2002) 65–75.
[5] D.A. Cowan, J.H. Brown, Effect of turbulence on limiting current in electrodialysis cells, Ind. Eng. Chem. 51 (1959) 1445–1448.
[6] I. Rubinstein, L. Shtilman, Voltage against current curves of cation exchange membranes, J. Chem. Soc., Faraday Trans. 2 (75) (1979) 231–246.
[7] R. Valerdi-Pérez, J. Ibáñez-Mengual, Current–voltage curves for an electrodialysis reversal pilot plant: determination of limiting currents, Desalination 141 (2001) 23–37.
[8] R. Ibanez, D.F. Stamatialis, M. Wessling, Role of membrane surface in concentration polarization at cation exchange membranes, J. Membr. Sci. 239 (2004) 119–128.
[9] G. Chamoulaud, D. Bélanger, Modification of ion-exchange membrane used for separation of protons and metallic cations and characterization of the membrane by current-voltage, J. Colloid. Interf. Sci. 281 (2005) 179–187.
[10] J.J. Krol, M. Wessling, H. Strathmann, Chronopotentiometry and overlimiting ion transport through monopolar ion exchange membranes, J. Membr. Sci. 162 (1999) 155–164.
[11] L. Marder, E.M. Ortega Navarro, V. Pérez-Herranz, A. Moura Bernardes, J. Zoppas Ferreira, Chronopotentiometric study on the effect of boric acid in the nickel transport properties through a cation-exchange membrane, Desalination 249 (2009) 348–352.
[12] J.J. Krol, M. Wessling, H. Strathmann, Concentration polarization with monopolar ion exchange membranes: current-voltage curves and water dissociation, J. Membr. Sci. 162 (1999) 145–154.
[13] N. Pismenskaya, V. Nikonenko, B. Auclair, G. Pourcelly, Transport of weak-electrolyte anions through anion exchange membranes: current–voltage characteristics, J. Membr. Sci. 189 (2001) 129–140.
[14] A. Ellatar, A. Elmidaoui, N. Pismemskaya, C. Gavach, G. Pourcelly, Comparison of transport properties of monovalent anions through anion-exchange membranes, J. Membr. Sci. 143 (1998) 249–261.
[15] Y. Tanaka, Limiting current density of an ion-exchange membrane and of an electrodialyzer, J. Membr. Sci. 266 (2005) 6–17.
[16] P. Sistat, G. Pourcelly, Chronopotentiometric response of an ion-exchange membrane in the underlimiting current-range. Transport phenomena within the diffusion layers, J. Membr. Sci. 123 (1997) 121–131.
[17] V.A. Shaposhnik, V.I. Vasil'eva, D.B. Praslov, Concentration fields of solutions under electrodialysis with ion-exchange membranes, J. Membr. Sci 101 (1995) 23–30.
[18] R. Kwaka, G. Guanb, W. Kung Pengb, J. Han, Microscale electrodialysis: Concentration profiling and vortex visualization, Desalination 308 (2013) 138–146.
[19] L. Beaulieu, J. Thibodeau, P. Bryl, M.É. Carbonneau, Characterization of enzymatic hydrolyzed snow crab [*Chionoecetes opilio*] by-product fractions: a source of high-valued biomolecules, Bioresour. Technol. 100 (2009) 3332–3342.
[20] A. Doyen, C. Roblet, L. Beaulieu, L. Saucier, Y. Pouliot, L. Bazinet, Impact of water splitting phenomenon during electrodialysis with ultrafiltration membranes on peptide selectivity and migration, J. Membr. Sci. 428 (2013) 349–356.
[21] F. Lin Teng Shee, J. Arul, S. Brunet, L. Bazinet, Chitosan solubilization by bipolar membrane electroacidification: reduction of membrane fouling, J. Membr. Sci. 290 (2007) 29–35.
[22] L. Bazinet, D. Ippersiel, C. Gendron, J. Beaudry, B. Mahdavi, J. Amiot, F. Lamarche, Cationic balance in skim milk during bipolar membrane electroacidification, J. Membr. Sci. 173 (2000) 201–209.
[23] Q. Wang, T. Ying, T. Jiang, D. Yang, M. Muzammil Jahangir, Demineralization of soybean oligosaccharides extract from sweet slurry by conventional electrodialysis, J. Food Eng. 95 (2009) 410–415.
[24] L. Firdaous, P. Dhulster, J. Amiot, A. Doyen, F. Lutin, L.P. Vézina, L. Bazinet, Investigation of the large-scale bioseparation of an antihypertensive peptide from alfalfa white protein hydrolysate by an electromembrane process, J. Membr. Sci. 355 (2010) 175–181.
[25] A. Doyen, L. Beaulieu, L. Saucier, Y. Pouliot, L. Bazinet, Demonstration of *in vitro* anticancer properties of peptide fractions from a snow crab by-products hydrolysate after separation by electrodialysis with ultrafiltration membranes, Sep. Purif. Technol. 78 (2011) 321–329.